Electronic Supplementary Material (ESI) for Chemical Communications

Supporting Information

Evidence that Steric Factors Modulate Reactivity of Tautomeric Oxo-Iron Species in Stereospecific Alkane C-H Hydroxylation

Mainak Mitra,[a] Julio Lloret-Fillol,[b] Matti Haukka,[c] Miquel Costas[b*], Ebbe Nordlander[a*]

[a]Department of Chemistry, Lund University, P.O.Box-124, Lund, SE-22100, Sweden
[b]QBIS Group, Department of Chemistry, University de Girona, Campus Montilivi, 17071 Girona, Catalonia, Spain
[c]Department of Chemistry, University of Jyväskylä, Jyväskylä, Finland

E-mail: Ebbe.Nordlander@chemphys.lu.se; miquel.costas@udg.edu.

Table of Contents

1. Experimental Section

Reagents and Materials:

Reagents and solvents were of at least 99% purity and used as received without any further purification. $H_2{}^{18}O_2$ (90% ^{18}O-enriched, 2% solution in $H_2{}^{18}O$) and $H_2{}^{18}O$ (95% ^{18}O-enriched) were received from ICON isotopes. All reagents and solvents were purchased from Sigma Aldrich or Fisher Scientific. Dichloromethane and acetonitrile were dried by distillation from CaH_2; diethyl ether was dried by distillation from Na/benzophenone. The starting material 4,7-dimethyl-1,4,7-triazacyclononane trihydrobromide (TACN:3HBr) was synthesized according to a literature procedure.[1]

Instrumentation:

Infrared spectra were collected on a Nicolet Avatar 360 FTIR spectrometer. UV-Visible spectroscopy was performed in a 1 cm quartz cell using an Agilent Technology 8453 UV-Vis spectrophotometer equipped with a diode-array detector. NMR spectra were recorded on a Bruker DPX 400 MHz spectrometer in $CDCl_3$ or CD_3CN solvent using standard conditions, and were referenced to the residual proton signal of the solvent. Elemental analysis was performed on an 4.1 Vario EL 3 elemental analyzer from Elementar. The ESI-MS experiments were performed with a Bruker esquire 6000 LC/MS chromatograph, using acetonitrile as a mobile phase. The product analyses after catalysis experiments were carried out on an Agilent Technology 7820A gas chromatograph with 16-sample automatic liquid sampler, flame ionization detector and EzChrom Elite Compact software. GC-MS analyses were performed on an Agilent Technology 7890A GC system equipped with 5975C inert XL EI/CI MSD with Triple-Axis Detector. The products were identified by comparison of their GC retention times and GC/MS with those of authentic compounds.

Syntheses

Synthesis of the ligand $^{Me2,\ BzIm}$TACN [1-(2-Methyl-1-benzimidazolyl)methyl-4,7-dimethyl-1,4,7-triazacyclononane]:

A total of 500 mg TACN:3HBr (1 eq., 1.25 mmol), 225.8 mg of 1-chloromethyl-2-methyl benzimidazole (1 eq., 1.25 mmol), 795 mg of Na_2CO_3 (6 eq., 7.5 mmol) and 20 mg of $(Bu)_4NBr$ (0.5 eq., 0.0625 mmol) were added to a 100 ml round bottom flask. To this mixture, 50 ml dry acetonitrile was added and the reaction mixture was refluxed under N_2 atmosphere for about 24 hr. After the reflux was finished, the reaction mixture was cooled down to room temperature and filtered through a celite pad. The celite pad was washed by a small amount of dichloromethane solvent. The filtrate was collected and evaporated and the resulting residue was washed with 1(M) NaOH solution. The organic part was extracted with dichloromethane, washed with brine solution and finally dried over anhydrous $MgSO_4$. The organic part was concentrated to a very small volume (5 ml) layered with hexane and kept overnight. Most of the ligand was extracted into the hexane part in very pure form. The hexane portion was collected and evaporated to give the pure ligand as an orange oil. Yield 228 mg (60%). ESI-MS (m/z) 302.2 $[M+H]^+$; NMR ^{1}H (400 MHz, $CDCl_3$) δ (ppm) 7.68 (d, J = 7.5 Hz, 1H), 7.34-7.22 (m, 3H), 4.01 (s, 2H), 3.87 (s, 3H), 2.99-2.85 (m, 12H), 2.47 (s, 6H); ^{13}C (100 MHz) δ (ppm) 152.37, 142.18, 136.23, 122.74, 122.15, 119.57, 109.34, 55.6, 55.56, 54.99, 45.92, 30.346.

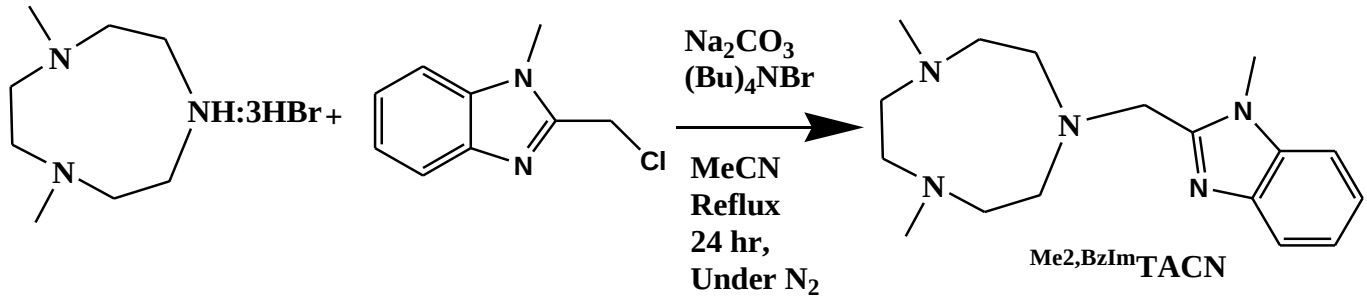

Scheme 1. Synthesis of the ligand $^{Me2,\ BzIm}$TACN

Synthesis of $[Fe^{II}(^{Me2,BzIM}TACN)(OTf)_2]$ (1^{OTf}):

A total of 0.436 gm of $[Fe^{II}(CH_3CN)_2(OTf)_2]$ (1 mmol) was dissolved in small amount (1 ml) of dichloromethane. To this solution, 0.3 gm of $^{Me2,\ BzIm}$TACN (1 eq., 1 mmol) in 1 ml dichloromethane was added under stirring. The reaction was performed inside a dry atmosphere box. A precipitate appeared within 30 min of stirring and the stirring was continued overnight. Then diethyl ether was added to the reaction mixture and the solid product was isolated by decantation of the solvent. The solid product was dried under high vacuum and finally isolated as a white powder. Yield 0.515 gm (79%). ESI-MS (m/z) 178.5 $[Fe^{II}(^{Me2,BzIM}TACN)]^{2+}$ (z = +2), calc. 178.5; 506.2 $[Fe^{II}(^{Me2,BzIM}TACN)(OTf)]^{+}$ (z = +1), calc. 506.2; Elemental analysis $C_{21}H_{30}F_6N_6O_6S_2Fe$ (MW = 696.46 g/mol) Calc. (%) C 36.21, H 4.34, N 12.07, S 9.21; Found (%) C 36.7, H 4.27, N 12.55, S 9.09; FTIR (KBr) ν (cm^{-1}) 3449 (br), 2924 (m), 1638 (s), 1498 (m), 1459 (m), 1293 (s), 1254 (s), 1162 (s), 1032 (s), 805 (s), 758 (m), 638 (s), 576 (s), 514 (s); ^{1}H-NMR spectra (400 MHz, CD_3CN) δ (ppm) 109.98, 75.51, 37.26, 24.2, 12.86, 0.7; UV/Vis λ (nm) 215 (ε = 3215 $M^{-1}cm^{-1}$), 240 (ε = 3260 $M^{-1}cm^{-1}$), 251 (ε = 3030 $M^{-1}cm^{-1}$), 323 (ε = 316 $M^{-1}cm^{-1}$).

Characterization of complex $\mathbf{1}^{\mathbf{OTf}}$

ESI-MS of $\mathbf{1}^{\mathbf{OTf}}$

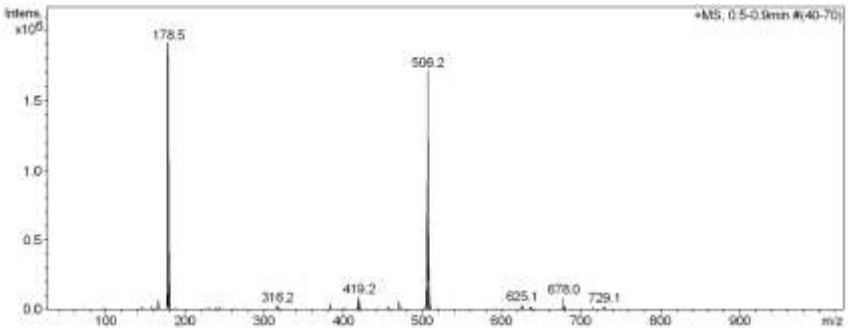

Figure S1. The ESI-MS of complex $\mathbf{1}^{\mathbf{OTf}}$. The mass peaks at m/z values 178.5 and 506.2 correspond to the formulations of $[Fe^{II}(^{Me2,BzIM}TACN)]^{2+}$ (z = +2) [calc. 178.5] and $[Fe^{II}(^{Me2,BzIM}TACN)(OTf)]^{+}$ (z = +1) [calc. 506.2], respectively.

^{1}H NMR spectra of **1**$^{\mathbf{OTf}}$

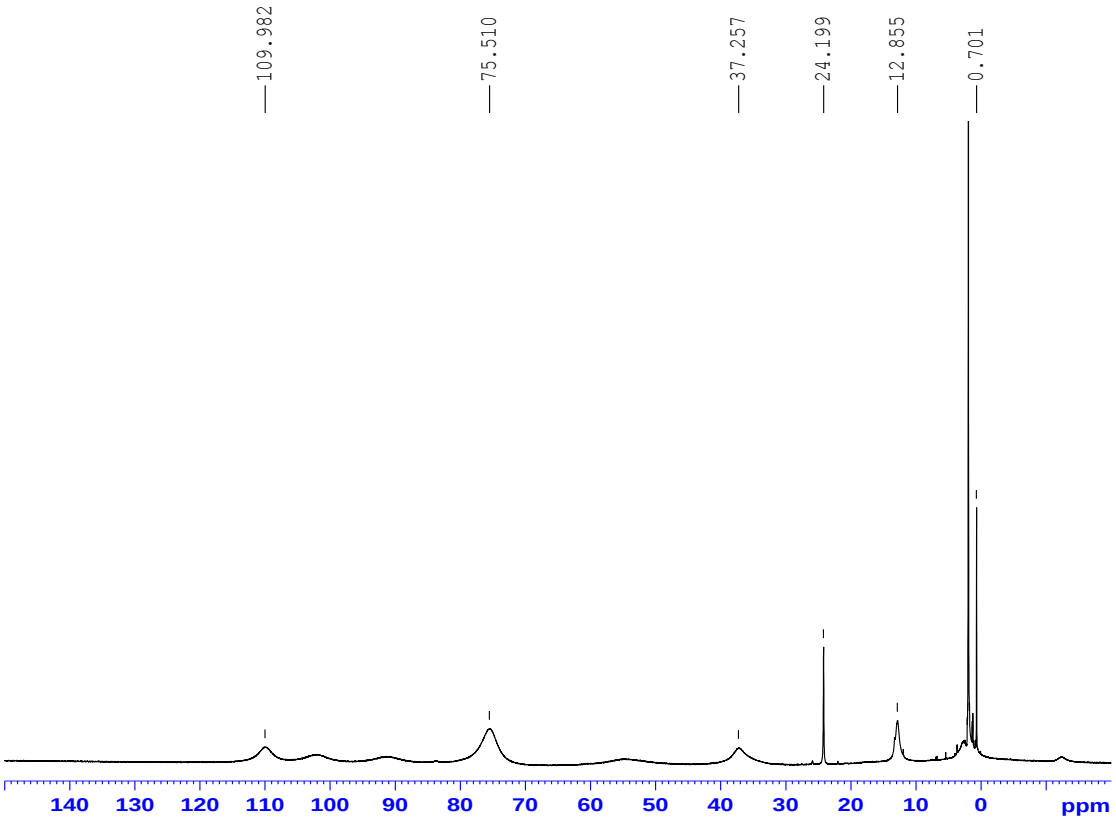

Figure S2. The ^{1}H NMR spectrum of complex **1**$^{\mathbf{OTf}}$ in CD_3CN.

UV/Vis spectrum of $\mathbf{1}^{\mathbf{OTf}}$.

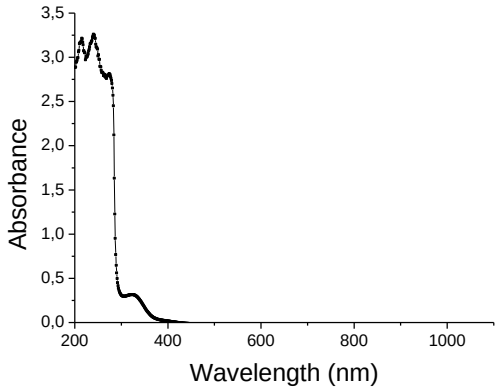

Figure S3. UV/Visible of 1 mM solution of complex $\mathbf{1}^{\mathbf{OTf}}$ in CH_3CN.

Crystallographic data collection for $[Fe^{II}(^{Me2,BzIM}TACN)(OTf)_2]$ (1^{OTf}) and $[Fe^{II}(^{Me2,BzIM}TACN)(OH)_2](OTf)_2$ (1^{H2O})

Crystal structure determination for complex 1^{OTf} . Crystals of 1^{OTf} were grown by slow diffusion of diethyl ether into a mixture of CH_2Cl_2:CH_3CN (5:1) solutions containing 1^{OTf}. The crystal was immersed in cryo-oil, mounted in a Nylon loop, and measured at a temperature of 298 K. The X-ray diffraction data were collected on a *BRUKER SMART APEX CCD* diffractometer using graphite-monochromated Mo *Kα* radiation (λ = 0.71073 Å). For data collections, the Smart[2] program was used and for data reductions, Saint+[3] program was used. The structure was solved by direct method and the refined by full-matrix least-squares methods on F^2. Structure solution and refinement was done using the SHELXTL[4] program. An empirical absorption correction (SADABS[5]) was applied to all data.

Crystal structure determination for complex 1^{H2O} . Crystals of 1^{H2O} were grown by slow diffusion of diethyl ether into a mixture of inert CH_2Cl_2:CH_3CN (5:1) containing 1^{OTf}. The crystal was immersed in cryo-oil, mounted in a MiTeGen loop, and measured at a temperature of 123 K. The X-ray diffraction data was collected on an Agilent Technologies Supernova diffractometer using Cu Kα radiation (λ = 1.54184 Å). The *CrysAlisPro*[6] program package was used for cell refinements and data reductions. The structure was solved by the charge flipping method using the *SUPERFLIP*[7] program with the *Olex2*[8] and *SHELXLE*[9] graphical user interfaces. A multi-scan absorption correction based on equivalent reflections (*CrysAlisPro*) was applied to the data. Structural refinement was carried out using *SHELXL-2013*.[10] The H_2O hydrogen atoms were located from the difference Fourier map but constrained to ride on their parent atom, with U_{iso} = 1.5·U_{eq}(parent atom). Other hydrogen atoms were positioned geometrically and constrained to ride on their parent atoms with C-H = 0.95–0.99 Å and U_{iso} = 1.2-1.5·U_{eq}(parent atom).

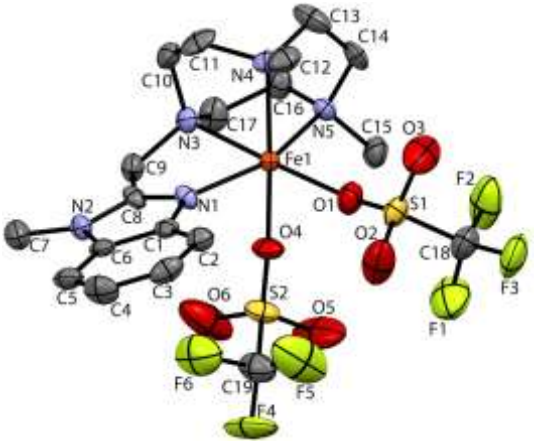

Figure S4. The molecular structure of $\mathbf{1}^{\mathbf{OTf}}$ with 30% probability ellipsoids. The hydrogen atoms have been omitted for clarity.

Table S1. Crystal data for $\mathbf{1}^{\mathbf{OTf}}$ and $\mathbf{1}^{\mathbf{H2O}}$

Empirical formula	$C_{19}H_{27}F_6FeN_5O_6S_2$	$C_{19}H_{31}F_6FeN_5O_8S_2$
	$\mathbf{1}^{\mathbf{OTf}}$	$\mathbf{1}^{\mathbf{H2O}}$
Formula weight	655.43	691.46
Temperature	298(2) K	123(2) K
Wavelength	0.71073 Å	1.54184 Å
Crystal system	Orthorhombic	Orthorhombic
Space group	$P2_12_12_1$	Pbca
Unit cell dimensions	a = 9.7786(15) Å	a = 16.1902(6) Å
	b = 15.903(3) Å	b = 15.4925(5) Å
	c = 17.253(3) Å	c = 22.7717(8) Å
	α = 90°	α = 90°
	β = 90°	β = 90°
	γ = 90°	γ = 90°
Volume	2682.9(7) $Å^3$	5711.7(3) $Å^3$
Z	4	8
Density (calculated)	1.623 Mg/m^3	1.608 Mg/m^3
Absorption coefficient	0.804 mm^{-1}	6.436 mm^{-1}
F(000)	1344	2848
Crystal size	0.20 x 0.08 x 0.05 mm^3	0.069 x 0.060 x 0.034 mm^3
Theta range for data collection	1.74 to 27.50 °	3.882 to 76.721°.
Index ranges	-12<=h<=12, -20<=k<=20, -22<=l<=22	-20<=h<=18, -19<=k<=11, -28<=l<=26
Reflections collected	41111	21092
Independent reflections	6172	5935 [R(int) = 0.0418]
Completeness	100.0 % (to theta = 27.50°)	99.8 % (to theta = 67.684°)
Absorption correction	Empirical	Semi-empirical from equivalents

Max. and min. transmission	1.0 and 0.784032	0.7540 and 0.6191
Refinement method	Full-matrix least-squares on F^2	Full-matrix least-squares on F^2
Data / restraints / parameters	6172 / 0 / 355	5935 / 0 / 375
Goodness-of-fit on F^2	1.164	1.021
Final R indices [I>2sigma(I)]	R1 = 0.1130, wR2 = 0.1598	R1 = 0.0447, wR2 = 0.1078
R indices (all data)	R1 = 0.2014, wR2 = 0.1883	R1 = 0.0604, wR2 = 0.1178
Largest diff. peak and hole	0.561 and -0.374 e.Å^{-3}	0.424 and -0.390 e.Å^{-3}

Table S2. Selected bond lengths (Å) and bond angles (°) for **1**$^{\mathbf{OTf}}$

Fe(1)-O(1)	2.076(6)
Fe(1)-N(1)	2.134(7)
Fe(1)-O(4)	2.147(5)
Fe(1)-N(4)	2.202(7)
Fe(1)-N(3)	2.219(8)
Fe(1)-N(5)	2.221(7)
O(1)-Fe(1)-N(1)	105.1(3)
O(1)-Fe(1)-O(4)	89.1(3)
N(1)-Fe(1)-O(4)	89.0(3)
O(1)-Fe(1)-N(4)	99.1(3)
N(1)-Fe(1)-N(4)	96.3(3)
O(4)-Fe(1)-N(4)	168.7(3)
O(1)-Fe(1)-N(3)	176.8(3)
N(1)-Fe(1)-N(3)	78.0(3)
O(4)-Fe(1)-N(3)	90.3(3)
N(4)-Fe(1)-N(3)	81.1(3)
O(1)-Fe(1)-N(5)	97.0(3)
N(1)-Fe(1)-N(5)	157.8(3)
O(4)-Fe(1)-N(5)	90.2(3)
N(4)-Fe(1)-N(5)	81.1(3)
N(3)-Fe(1)-N(5)	79.8(3)

Table S3. Selected bond lengths (Å) and bond angles (°) for $\mathbf{1}^{H2O}$

Fe(1)-O(1)	2.113(2)
Fe(1)-N(1)	2.132(2)
Fe(1)-O(2)	2.148(2)
Fe(1)-N(3)	2.214(2)
Fe(1)-N(4)	2.222(2)
Fe(1)-N(2)	2.248(2)
O(1)-Fe(1)-N(1)	104.83(9)
O(1)-Fe(1)-O(2)	89.16(8)
N(1)-Fe(1)-O(2)	86.40(8)
O(1)-Fe(1)-N(3)	98.90(9)
N(1)-Fe(1)-N(3)	156.27(9)
O(2)-Fe(1)-N(3)	93.34(9)
O(1)-Fe(1)-N(4)	96.77(9)
N(1)-Fe(1)-N(4)	98.01(9)
O(2)-Fe(1)-N(4)	171.42(9)
N(3)-Fe(1)-N(4)	79.65(9)
O(1)-Fe(1)-N(2)	176.99(9)
N(1)-Fe(1)-N(2)	76.79(9)
O(2)-Fe(1)-N(2)	93.50(8)
N(3)-Fe(1)-N(2)	79.54(9)
N(4)-Fe(1)-N(2)	80.43(9)

Reaction Conditions for Catalysis Experiments

In a typical reaction, 360 µL of H_2O_2 (25 µmol) taken from a 70 mM H_2O_2 stock solution in CH_3CN together with 45 µL of water (2500 µmol) was delivered by syringe pump over 30 min at room temperature under air to a vigorously stirred CH_3CN solution (2.14 ml) containing the Fe-catalyst (2.5 µmol) and the alkane substrate (2500 µmol). The final concentrations were 1 mM for catalyst, 10 mM for the oxidant, 1000 mM for H_2O and 1000 mM for substrate (1:10:1000:1000 for cat:ox:H_2O:sub). For adamantane, due to the low solubility, only 50 µmol of the substrate was used and so the final concentration for it was 20 mM. At the conclusion of the syringe pump addition, 500 µL of a biphenyl solution of a known concentration (~25 mM) was added to the reaction mixture as internal standard. The reaction mixture was then passed through a small silica column (to remove the iron complex), followed by elusion with 2 ml ethyl acetate. Finally the solution was subjected to GC analysis. The organic products were identified and their yields were calculated by using authentic compounds.

For the measurement of kinetic isotope effects (KIE), a substrate mixture of cyclohexane:cyclohexane-d_{12} in a ratio of 1:3 was used to improve the accuracy of the obtained KIE value.

Isotope Labeling Studies

Catalytic reaction conditions using $H_2{}^{18}O$: In a typical reaction, 290 µL of H_2O_2 (20 µmol) taken from a 70 mM H_2O_2 stock solution in CH_3CN was delivered by syringe pump over 30 min at room temperature under air to a vigorously stirred CH_3CN solution (1.71 ml) containing the Fe-catalyst (2.0 µmol), substrate (2000 µmol) and $H_2{}^{18}O$ (2000 µmol). The final concentrations were 1 mM for catalyst, 10 mM of the oxidant, 1000 mM for $H_2{}^{18}O$ and 1000 mM for substrate (1:10:1000:1000 for cat:H_2O_2:$H_2{}^{18}O$:subs). For adamantane, due to the low solubility, only 50 µmol of the substrate was used and so the final concentration for it was 20 mM.

Catalytic reaction conditions using $H_2{}^{18}O_2$: In a typical reaction, 34 µL of $H_2{}^{18}O_2$ (20 µmol) taken from a 2% (wt/wt) $H_2{}^{18}O_2$ solution in $H_2{}^{18}O$ was delivered by syringe pump over 30 min at room temperature under air to a vigorously stirred CH_3CN solution (2 ml) containing the Fe-catalyst (2.0 µmol), substrate (2000 µmol) and 45 µL of H_2O. The final concentrations were 1 mM for catalyst, 10 mM for the oxidant, 1000 mM for H_2O and 1000 mM for substrate (1:10:1000:1000 for cat:$H_2O_2{}^{18}$:H_2O:sub).

In the oxidation of adamantane and cis-1,2-dimethylcyclohexane, the solution (after syringe pump addition) was passed through a small silica column to remove the Fe-catalyst, followed by elution with 2 ml ethyl acetate. For other substrates, the reaction solution was treated with 1 ml acetic anhydride and 0.1 ml of 1-methylimidazole to esterify the alcohol products for GC-MS analyses (tertiary alcohols are not esterified under these conditions). Samples were concentrated by removing part of the solvent under vacuum and subjected to GC-MS analyses.

2. Catalysis results

(A) Oxidation of different alkane substrates by **1**$^{\mathbf{OTf}}$

Table S4. Catalytic oxidation of alkanes by **1**$^{\mathbf{OTf}}$ using H_2O_2 as a co-oxidant. Condition 1:10:1000:1000 cat:H_2O_2:H_2O:sub; CH_3CN, air, room temp.

Substrate	TN (A)[a]	TN (K)[b]	A/K[c]	Yield (%)[d]
Cyclohexane	8.5	0.8	10.6	93
Cyclohexane-d_{12}	5.5	0.5	11	60
Cyclooctane	6	0.9	68.8	6.8
n-Hexane	4	0.8	5	48.4
2,3-dimethylbutane	2.8	---	---	31.6

a) TN (A): TN of alcohol product (cyclohexanol, cyclohexanol-d_{11}, cyclooctanol, 2- and 3-hexanol, 2,3-dimethylbutanol) = (mol of alcohol)/(mol of catalyst).

b) TN (K): TN of ketone product (cyclohexanone, cyclohexanone-d_{11}, cyclooctanone, 2- and 3-hexanone) = (mol of ketone)/(mol of catalyst).

c) A/K = (mol of alcohol)/(mol of ketone).

d) % Yield = (mol of alcohol + mol of ketone)/(mol of oxidant) x 100.

Table S5. Oxidation of cis-1,2-dimethylcyclohexane (cis-DMCH) by $\mathbf{1}^{\mathbf{OTf}}$ using H_2O_2 as a co-oxidant. Condition 1:10:1000:1000 cat:H_2O_2:H_2O:sub; CH_3CN, air, room temp.

Substrate	TN (1R,2R + 1S,2S)[a]	TN (1R,2S + 1S,2R)[b]	RC (%)[c]	Yield (%)[d]
cis-1,2-dimethylcyclohexane	4.9	0.08	97	49.6

a) TN (1R,2R + 1S,2S): TN of the two enantiomers of cis-1,2-dimethylcyclohexanol = (mol of cis-ol)/(mol of catalyst).

b) TN (1R,2S + 1S,2R): TN of the two enantiomers of trans-1,2-dimethylcyclohexanol = (mol of trans-ol)/(mol of catalyst).

c) RC: Retention of configuration in the oxidation of tertiary C-H bonds in cis-DMCH = [(1R,2R + 1S,2S)-(1R,2S + 1S,2R)]/[(1R,2R + 1S,2S)+(1R,2S + 1S,2R)].

d) % Yield = (mol of cis-ol + mol of trans-ol)/(mol of oxidant) x 100.

Table S6. Oxidation of adamantane by $\mathbf{1}^{\mathbf{OTf}}$ using H_2O_2 as a co-oxidant. Condition 1:10:1000:50 cat:H_2O_2:H_2O:sub; CH_3CN, air, room temp.

Substrate	TN (1-ol)[a]	TN (2-ol + 2-one)[b]	3°/2°[c]	Yield (%)[d]
Adamantane	3	0.64	14	36

a) TN (1-ol): TN of 1-adamantanol = (mol of 1-adamantanol)/(mol of catalyst).

b) TN (2-ol + 2-one): TN of 2-adamantanol and 2-adamantanone = (mol of 2-adamantanol + mol of 2-adamantanone)/(mol of catalyst).

c) 3°/2° = 3 x [1-ol/(2-ol + 2-one)].

d) % Yield = (mol of 1-ol + mol of 2-ol and 2-one)/(mol of oxidant) x 100.

(B) Oxidation of olefins by $\mathbf{1}^{\mathbf{OTf}}$

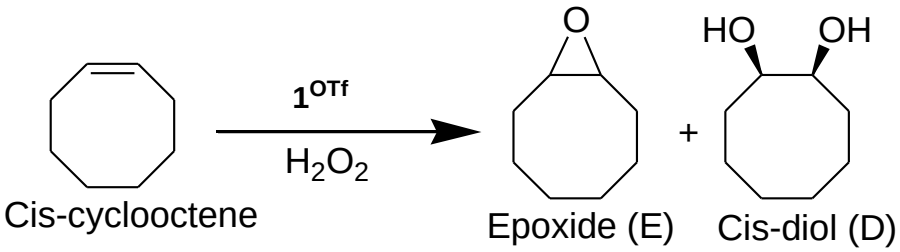

Table S7. Oxidation of cis-cyclooctene by $\mathbf{1}^{\mathbf{OTf}}$ using H_2O_2 as a co-oxidant in CH_3CN under air at room temp.

Cat:H_2O_2:sub	TN[a] of E[b]	TN[a] of D[c]	Total TN (D + E)	D/E[d]	Conversion of substrate (%)[e]
1:100:1000	26.4	56.8	83.2	2.1	84
1:100:100	24.1	39.3	63.4	1.6	89
1:120:100	27	40.8	67.8	1.5	82

(a) TN = (mol product)/(mol catalyst)

(b) E = cyclooctene epoxide

(c) D = cis-cycloctanediol

(d) D/E = (mol of cis-diol)/(mol of epoxide)

(e) Conversion with respect to oxidant

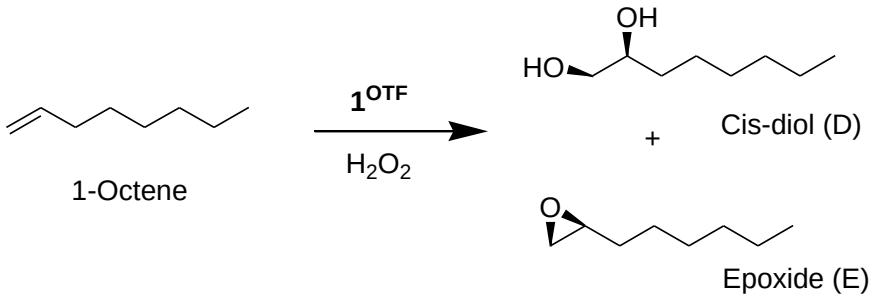

Table S8. Oxidation of 1-octene by **1**^{OTf} using H_2O_2 as a co-oxidant in CH_3CN under air at room temp.

Cat:H_2O_2:sub	TN[a] of E[b]	TN[a] of D[c]	Total TN (D + E)	D/E[d]
1:100:1000	17.9	85.8	103.7	4.8
1:100:100	10.5	37	47.5	3.5
1:120:100	12.3	40.7	41	3.3

(a) TN = (mol product)/(mol catalyst)

(b) E = 1-octane epoxide

(c) D = cis-octane-1,2-diol

(d) D/E = (mol of cis-diol)/(mol of epoxide)

3) Time Course Study

The time course oxidation of cyclohexane by $\mathbf{1}^{\mathbf{OTf}}$ with H_2O_2 was followed.

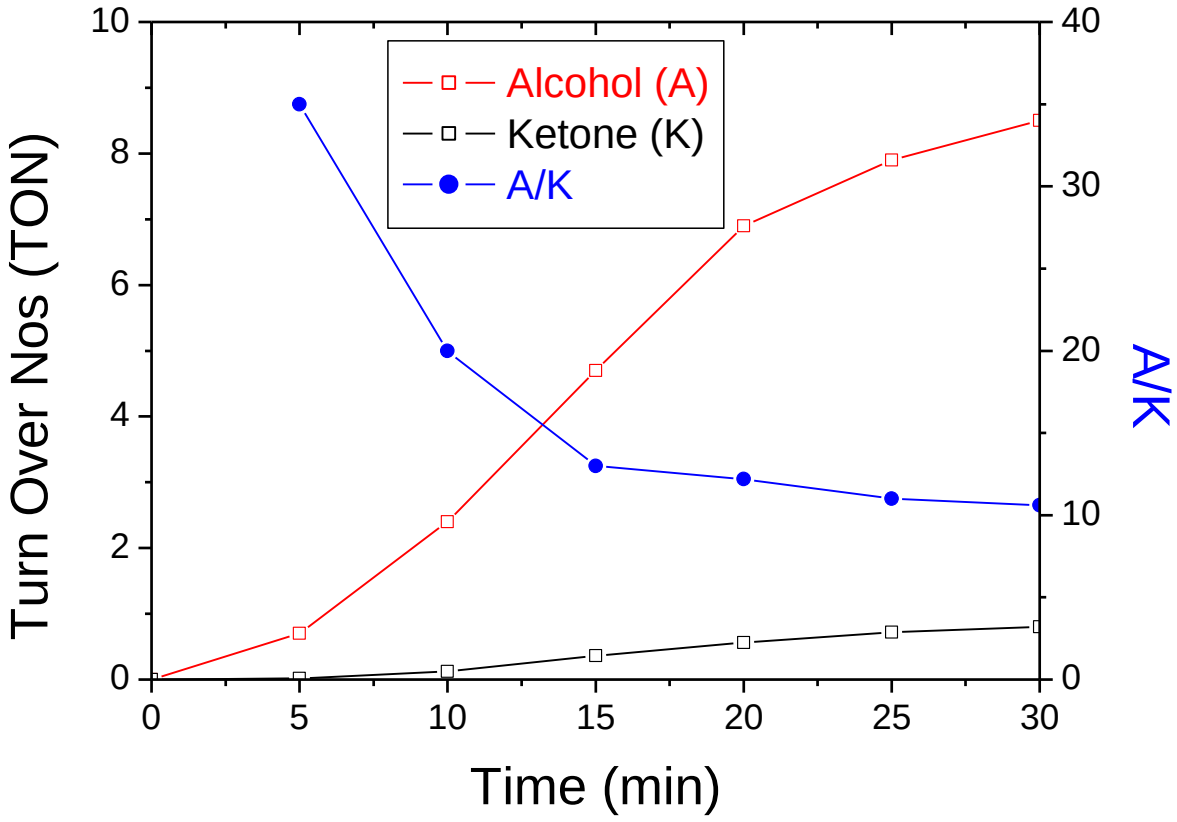

Figure S5. Time course oxidation of cyclohexane in presence of H_2O_2 catalyzed by $\mathbf{1}^{\mathbf{OTf}}$.

4) Comparison of Catalytic Conversion in the Oxidation of Cyclohexane Mediated by 1^{OTf} with some other reported Fe(II) complexes

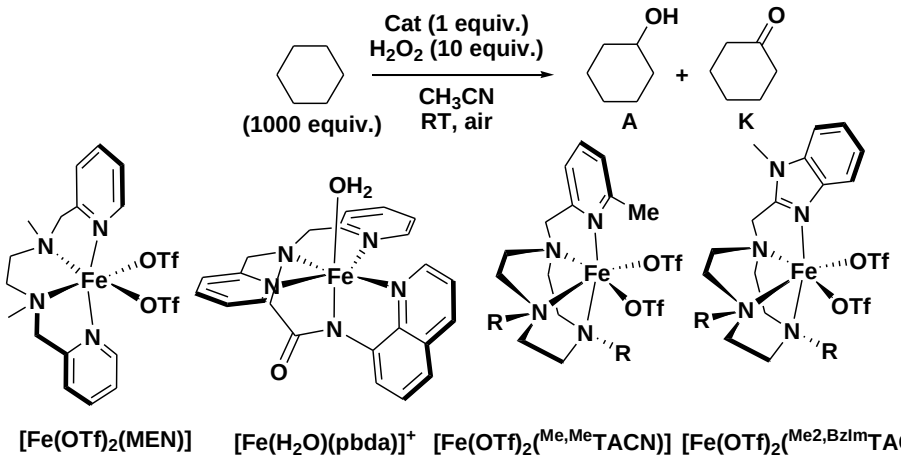

Scheme 2). Comparison of catalytic conversion in the oxidation of cyclohexane by different Fe(II)-catalysts using H_2O_2 as a co-oxidant.

6.3	15.6[a]	7.6	9.3	**TON (A+K)**
71	78	84	(99-100)	**Efficiency (%)**
8	11.3	10	10.6	**A/K**
11	12	13	This work	**Reference**

(a) 20 eqv. H_2O_2 was added.

5) Results of Isotope Labeling Experiments

% of ^{18}O labeled cyclohexanol v/s [$H_2{}^{18}O$]

Table S9. Percentage of ^{18}O incorporation into cyclohexanol (% $R^{18}OH$) in oxidation of cyclohexane by $\mathbf{1}^{\mathbf{OTf}}$ in presence of H_2O_2 (10 equivalents) and $H_2{}^{18}O$

Entry	Equivalents of $H_2{}^{18}O$	[$H_2{}^{18}O$] in M	% of $R^{18}OH$
1	50	0.05	26.6
2	100	0.1	34.5
3	250	0.25	40.4
4	600	0.6	46
5	1000	1.0	47.6
6	1200	1.2	47.7

Reaction conditions for catalysis: 0.29 mL (20 µmol) of H_2O_2 (70 mM) solution together with appropriate amount of $H_2{}^{18}O$ was delivered by syringe pump over 30 min under air at room temperature to a CH_3CN solution (1.71 mL) containing the Fe-catalyst (2 µmol) and the substrate (2000 µmol).

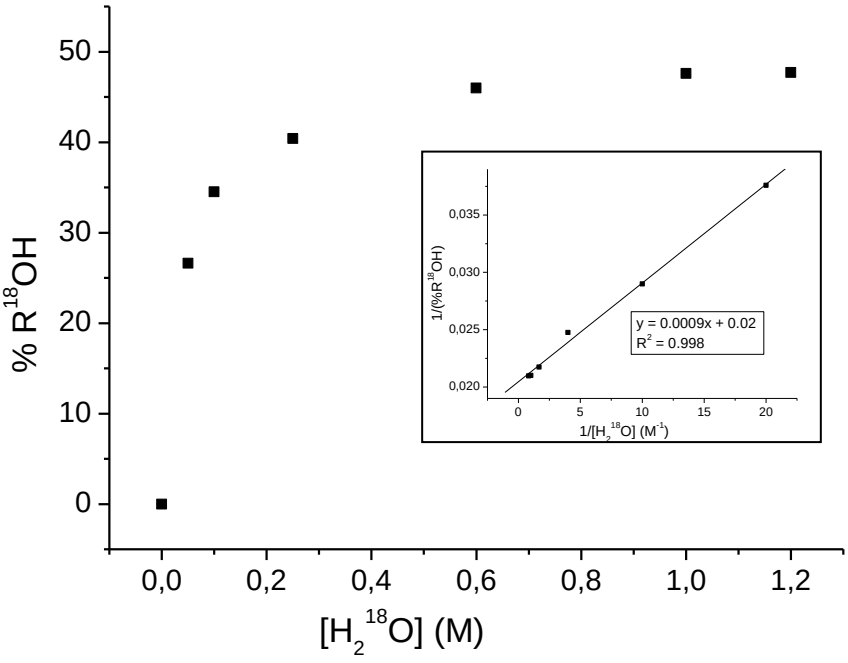

Figure S6. Fraction of ^{18}O-labeled cyclohexanol (% $R^{18}OH$) v/s concentration of $H_2{}^{18}O$. Inset: double reciprocal plot.

% of ^{18}O-labeled alcohol v/s [cis-1,2-dimethylcyclohexane]

Table S10. Percentage of ^{18}O-incorporation in the alcohol product ($R^{18}OH$) in the oxidation of different equivalents of cis-1,2-cyclohexane by $\mathbf{1}^{\mathbf{OTf}}/H_2O_2$

Catalyst (Eqv.)	H_2O_2 (Eqv.)	$H_2{}^{18}O$ (Eqv.)	Equivalents of substrate	% of $R^{18}OH$
1	10	1000	50	26.6
2	10	1000	100	26.4
3	10	1000	250	25.6

Reaction condition for catalysis: 0.29 mL (20 µmol) of H_2O_2 (70 mM) solution together with 40 µL of $H_2{}^{18}O$ (2000 µmol) was delivered by syringe pump over 30 min under air at room temperature to a CH_3CN solution (1.71 mL) containing the Fe-catalyst (2 µmol) and the appropriate amount of the substrate (50-250 equivalents).

Control experiments were performed by determining ^{18}O incorporation from $H_2{}^{18}O$ into cyclohexanol in a set of cyclohexane oxidation reactions catalyzed by $\mathbf{1}^{\mathbf{OTf}}$, and where [$H_2{}^{18}O$] was systematically modified. It was found that the extent of ^{18}O-label incorporation increased linearly with [$H_2{}^{18}O$] at lower concentration of the latter but showed a plateau at higher concentration (Table S9 and Figure S6). These observations suggest that a pre-equilibrium consisting of reversible coordination of water precedes formation of the ^{18}O-hydroxylating species, and ensured that at 1000 equiv of $H_2{}^{18}O$ the system is fully saturated. Furthermore, the level of incorporation was found to be independent of substrate concentration (Table S10).

6) References:

1. C. Flassbeck and K. Wieghardt, *Z. Anorg. Allg. Chem.*, 1992, **608**, 60-68.
2. Bruker Advanced X-ray Solutions. SMART: Version 5.631, 1997-2002.
3. Bruker Advanced X-ray Solutions. SAINT +, Version 6.36A, 2001.
4. G. M. Sheldrick, *Empirical Absorption Correction Program*, Universität Göttingen, 1996.
5. Bruker Advanced X-ray Solutions. SADABS Version 2.10, 2001.
6. Agilent, *CrysAlisPro*, Agilent Technologies inc., 2013, Yarnton, Oxfordshire, England.
7. Palatinus, L.; Chapuis, G. *J. Appl. Cryst.* **2007**, *40*, 786-790.
8. O. V. Dolomanov, L. J. Bourhis, R. J. Gildea, J. A. K. Howard and H. J. Puschmann, *J. Appl. Cryst.*, 2009, **42**, 339-341.
9. C. B. Hübschle, G. M. Sheldrick and B. Dittrich, *J. Appl. Cryst*,. 2011, **44**, 1281-1284.
10. G. M. Sheldrick, *Acta Cryst.*, 2008, **A64**, 112-122.
11. K. Chen and L. Que Jr., *J. Am. Chem. Soc.*, 2001, **123**, 6327-6337.
12. Y. Hitomi, K. Arakawa, T. Funabiki and M. Kodera, *Angew. Chem. Int. Ed.*, 2012, **51**, 3448-3452.
13. A. Company, L. Gomez, X. Fontrodona, X. Ribas and M. Costas, *Chem. Eur. J.*, 2008, **14**, 5727-5731.